TOOLS AND RESOURCES

A point mutation in human coilin prevents Cajal body formation

Davide A. Basello[1,2], A. Gregory Matera[3] and David Staněk[1,*]

ABSTRACT

Coilin is a conserved protein essential for integrity of nuclear membrane-less inclusions called Cajal bodies. Here, we report an amino acid substitution (p.K496E) found in a widely-used human EGFP–coilin construct that has a dominant-negative effect on Cajal body formation. We show that this coilin-K496E variant fails to rescue Cajal bodies in cells lacking endogenous coilin, whereas the wild-type construct restores Cajal bodies in mouse and human coilin-knockout cells. In cells containing endogenous coilin, both the wild-type and K496E variant proteins accumulate in Cajal bodies. However, high-level overexpression of coilin-K496E causes Cajal body disintegration. Thus, a mutation in the C-terminal region of human coilin can disrupt Cajal body assembly. Caution should be used when interpreting data from coilin plasmids that are derived from this variant (currently deposited at Addgene).

KEY WORDS: Coilin, Cajal bodies, Mutation

INTRODUCTION

Cajal bodies (CBs) are subnuclear domains that were discovered over a century ago (Cajal, 1903). Numerous short non-coding (nc) RNAs accumulate in CBs, and there is ongoing debate regarding the role of CBs in ncRNA and ribonucleoprotein metabolism (reviewed in Stanek, 2017). A seminal finding in this research area was the discovery of coilin (Andrade et al., 1991), a protein that has become the primary marker of CBs. Coilin is also a scaffolding protein essential for CB integrity in all organisms tested to date (Chen et al., 2015; Collier et al., 2006; Liu et al., 2009; Stern et al., 2012; Strzelecka et al., 2010; Tucker et al., 2001). Coilin was first identified using antibodies present in human autoimmune patient sera (Raška et al., 1991). Subsequently, Tan and colleagues generated a partial cDNA clone, encoding the C-terminal 405 amino acids (aa) of coilin (Andrade et al., 1991). Later, Gall and colleagues created the first plasmid containing all 576 aa of human coilin and characterized the N-terminal self-association domain (Wu et al., 1994). At the same time, Roth and his co-workers identified coilin in frog (Tuma et al., 1993). Hebert and Matera re-cloned Wu's original plasmid, tagged coilin with EGFP and also identified and cloned the mouse and zebrafish coilin genes, allowing identification of conserved N- and C-terminal regions (Hebert and Matera, 2000; Shpargel et al., 2003; Tucker et al., 2000). Thanks to 30 years of community effort, we now know that coilin can be divided into three functional regions. The N-terminus

[1]Institute of Molecular Genetics, Czech Academy of Science, Prague, Czech Republic. [2]Faculty of Science, Charles University, Prague 14220, Czech Republic. [3]Integrative Program for Biological and Genome Sciences, and Department of Biology, University of North Carolina, Chapel Hill, NC 27599-3280, USA.

*Author for correspondence (stanek@img.cas.cz)

D.S., 0000-0002-5865-175X

is predicted to fold into a globular domain and provides the platform for coilin self-interaction. The C-terminal carries an atypical Tudor domain and interacts with small nuclear ribonucleoprotein (snRNP)-specific Sm proteins (Hebert and Matera, 2000; Shanbhag et al., 2010; Toyota et al., 2010; Wu et al., 1994; Xu et al., 2005). The N- and C-terminal domains are connected by a long, likely unstructured region (Fig. 1A). This linker domain features two nuclear localization signal (NLS) sequences, a putative nucleolar localization signal (NoLS) and an arginine and glycine-rich region (RG-box), that is recognized by the SMN protein (Chan et al., 1994; Hebert et al., 2001; Machyna et al., 2015; Tucker et al., 2000; Tuma et al., 1993).

Both coilin N- and C-termini have been implicated in proper assembly of CBs. The N-terminus of coilin is necessary and sufficient for localization to extant CBs (Hebert and Matera, 2000; Wu et al., 1994). The C-terminus was thought to play a regulatory role, as human coilin failed to rescue CB formation in coilin-null mouse embryonic fibroblasts (MEF$^{coilin-/-}$) (Shpargel et al., 2003). A more detailed analysis of chimeric coilin constructs revealed that the C-terminal domain of the human protein was the region that prevented CB assembly in mouse knockout (KO) cells (Shpargel et al., 2003). It was speculated that post-transcriptional modifications and sequence differences at the very C-terminus regulated CB assembly (Shpargel et al., 2003; Tapia et al., 2010; Toyota et al., 2010).

We noticed that a plasmid containing human coilin cDNA deposited in Addgene (#36906) contains three point mutations. Two of these mutations are silent but the third mutation leads to the replacement of lysine 496 with glutamic acid. In this manuscript, we analyzed coilin^{K496E} and showed that this coilin variant is unable to rescue CB formation in mouse and human cells lacking endogenous coilin and has a dominant negative effect on CB formation in cells expressing wild-type (WT) coilin.

RESULTS

We analyzed the sequence of the original tagged version of human EGFP–coilin annotated in Addgene (#36906) and found that it differed at three positions from the sequence of human coilin annotated in GenBank (NCBI reference sequence NM_004645.3). Specifically, we identified two silent mutations c.784A>G (p.E251E) and c.1642C>T (p.A537A) and more importantly, a third mutation c.1517A>G that leads to amino acid change in the C-terminal domain (p.K496E) (a graphical representation is shown in Fig. 1A). Lysine 496 is conserved in most species from human to Trichoplax and the 14-aa region around K496 is fully conserved in vertebrates, which suggests it has functional importance (Machyna et al., 2015). We sequenced a EGFP–coilin plasmid in our stock and identified the same mutations, which were most likely carried over from past re-cloning of the EGFP–coilin plasmid (Stanek and Neugebauer, 2004). Furthermore, Shanbhag et al. reported two of these mutations (p.A537A and p.K496E) in a plasmid encoding a portion of human coilin (320–576 aa) obtained from Hebert's laboratory (Shanbhag et al., 2010).
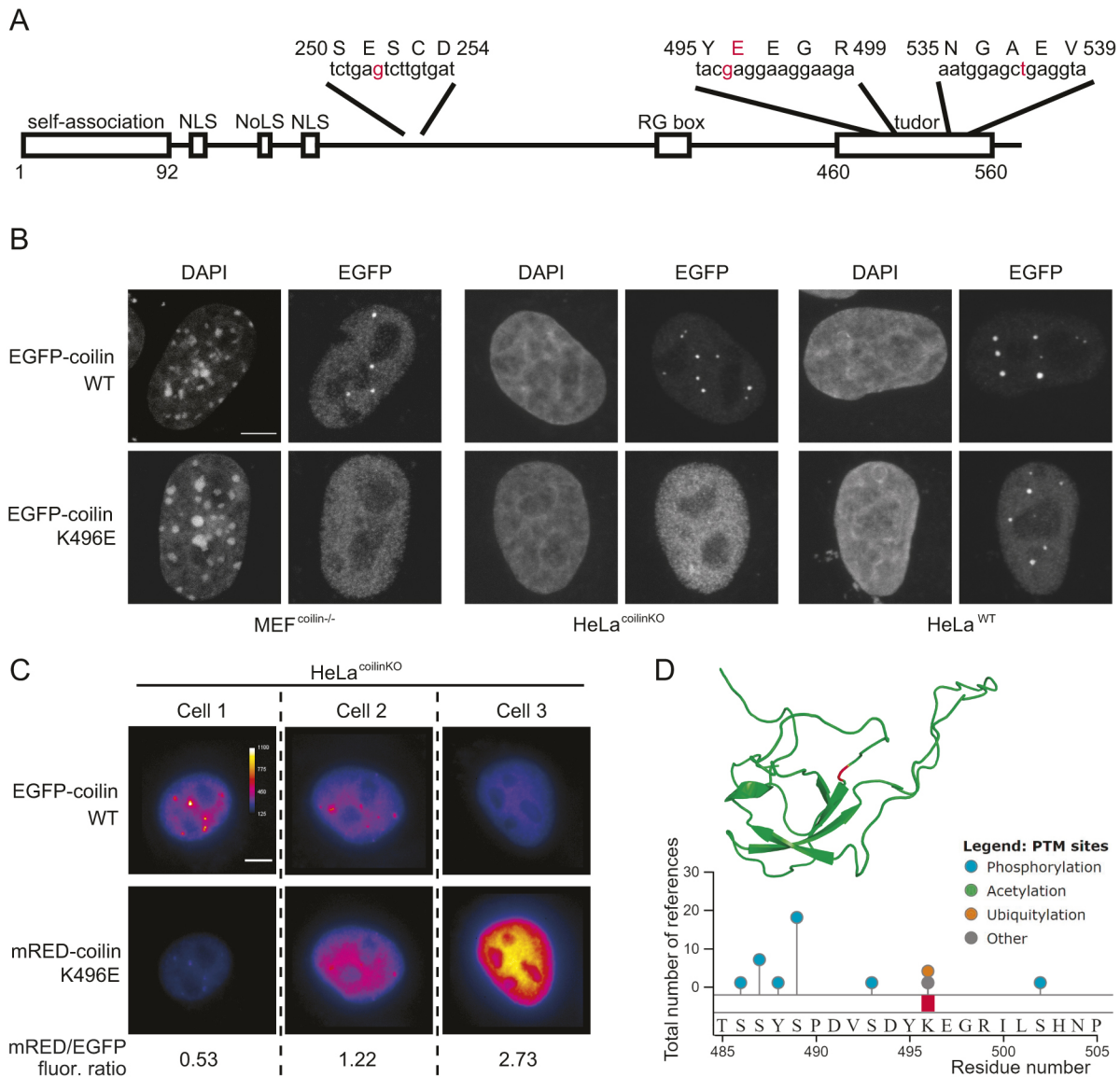
Fig. 1. A point mutation in coilin prevents Cajal body formation. (A) Schematic representation of coilin. The positions of point mutations in the Addgene construct #36906 are shown and highlighted by red color in the context of coilin domains. (B) Transfection of MEF[coilin−/−] (left), HeLa[coilinKO] (center) and Hela[WT] (right) with EGFP–coilin[WT] or EGFP–coilin[K496E]. EGFP fluorescence and DNA staining with DAPI is shown. Images are representative of three experiments; for quantification of the proportion of cells with CB, see Fig. S1A. (C) Co-transfection of HeLa coilin[KO] cells by EGFP–coilin[WT] and mRED–coilin[K496E]. Three individual cells are presented; EGFP fluorescence shown in the top row and mRED fluorescence in the bottom row. Fluorescence of both fluorochromes is pseudocolored (mpl-inferno color map in ImageJ) to indicate the signal intensity. Color bar in the top left image displays fluorescence intensity and apply to both channels. Each cell expresses a different ratio of WT and K496E coilin, these differences in expression are indicated as the mRED/EGFP ratio underneath images. Images are representative of one experiment. (D) A structure of the C-terminal domain of coilin based on Shanbhag et al. (2010). The mutated K496 is marked red. Identified post-translation modifications of the coilin region comprising K496 is shown. Image was adapted from PhosphoSitePlus (www.phosphosite.org). Scale bars: 5 μm.

These findings suggest that a mutated form of coilin could have been used in the past, unknowingly reported as WT coilin, in different laboratories. More importantly, the effect of the K496E substitution on coilin function had not been determined. In order to address whether the K496E substitution influences CB formation, we reverted the mutation to WT condition by site-directed mutagenesis. We transfected both EGFP–coilin[WT] and EGFP–coilin[K496E] constructs (EGFP tag at the N-terminus of coilin) individually into MEF[coilin−/−] cells, which were originally used to interrogate this issue (Shpargel et al., 2003). In contrast to the original findings (Shpargel et al., 2003), we observed that human EGFP–coilin[WT] was able to reconstitute CBs when expressed in mouse knockout cells whereas no CBs formed in cells expressing EGFP–coilin[K496E] (Fig. 1B, left panels; Fig. S1A). To further examine the properties of this K496E missense mutant and to verify that our results were not limited to mouse cells, we expressed both coilin constructs in a human coilin KO cell line (HeLa[coilinKO]). Once again, CBs were present in cells transfected with human EGFP–coilin[WT], but no CBs were observed in cells expressing EGFP–coilin[K496E] (Fig. 1B, central panels; Fig. S1A). The same result was obtained when we expressed coilin[K496E] tagged with the triple FLAG tag at the N-terminus (Fig. S1B), demonstrating that the size of the tag did not influence coilin behavior (see also Hebert and Matera, 2000). We also monitored the distribution of two other

constituents of CB, spliceosomal snRNPs and fibrillarin. CBs formed in HeLa^{coilinKO} cells after expression of EGFP–coilin^{WT} contained both snRNPs (as detected by the anti-2,2,7-trimethyl guanosine antibody) and fibrillarin (Fig. S1C). snRNPs were distributed diffusely in the nucleoplasm with no obvious accumulation in CB-like structures in HeLa^{coilinKO} cells and this pattern did not change upon expression of EGFP–coilin^{K496E} protein (Fig. S1C,D). Fibrillarin was localized only to nucleoli in HeLa^{coilinKO} cells with no localization to any residual bodies even after expression of EGFP–coilin^{K496E} (Fig. S1C,D). These data strongly indicate a loss-of-function for the coilin-K496E variant. Interestingly, both constructs are able to accumulate in pre-formed CBs as demonstrated by transfection of parental HeLa cells (Fig. 1B, right panel). These findings are consistent with previously published data showing that the coilin N-terminus is necessary and sufficient for coilin localization to preexisting CBs (Bohmann et al., 1995; Hebert and Matera, 2000; Wu et al., 1994).

We noticed that CBs are not present in parental HeLa cells with high expression of EGFP–coilin^{K496E}. Accordingly, we observed a reduced proportion of cells with CBs when cells were transfected with EGFP–coilin^{K496E} construct compared to the proportion of cells expressing EGFP–coilin^{WT} (Fig. S1A, right graph). The expression of WT and mutated coilin was not significantly different (Fig. S1E), which shows that the effect is not due to a different amount of expressed coilin protein but rather the presence of the mutated variant. We decided to further analyze whether the K496E variant affects CB formation in individual cells. We transfected different amounts of EGFP–coilin^{WT} together with mRED–coilin^{K496E} in HeLa^{coilinKO} cells. We observed a negative correlation between the mRED/EGFP fluorescence ratio and CB presence (Fig. 1C). These data show that high-level overexpression of the K496E variant had a dominant negative effect on assembly of WT coilin in CBs. Similarly, overexpression of a truncated version of coilin composed of the N-terminal 92 aa has been previously shown to disrupt CBs (Hebert and Matera, 2000).

Finally, we monitored dynamics of both coilin variants in CBs by fluorescence recovery after photobleaching (FRAP). Both EGFP–coilin variants were expressed in HeLa^{WT} cells and fluorescence recovery was measured after photobleaching of EGFP in CBs (Fig. S1F). EGFP–coilin^{K496E} showed faster recovery, which indicates that the K496E substitution reduces the residency time of coilin in CBs. However, we observed relatively large differences in recovery time between individual cells as indicated by elevated standard deviations, and the results should be taken with caution.

DISCUSSION

We identified a mutation in the C-terminal domain of coilin that negatively affects its ability to form CBs and shortens CB residency time. However, the molecular mechanism of how the K496E mutation alters coilin behavior is unclear. K496 is located just outside the Tudor-like domain and bridges this domain with a conserved loop (Shanbhag et al., 2010). Replacement of a basic lysine residue with an acidic one might impact the loop flexibility and/or affect the folding of the Tudor-like domain. However, replacing the loop with a β-turn motif does not affect the folding of the central Tudor-like domain (Shanbhag et al., 2010). The C-terminal domain has been shown to interact with Sm proteins, but the molecular mechanism is unclear because detailed examination of Tudor-like domain interaction with methylated amino acids revealed no binding (Shanbhag et al., 2010; Xu et al., 2005). In addition to its inability to rescue CB formation, the coilin^{K496E} variant has a dominant-negative effect on CB integrity in cells

expressing endogenous coilin (Fig. 1C; Fig. S1A). Coilin forms oligomers and this ability is crucial for CB formation (Hebert and Matera, 2000). If the CB-disruptive variant coilin^{K496E} prevails in coilin oligomers, it likely changes behavior of the whole oligomer, which would then no longer be able to scaffold CBs.

K496 can be sumoylated (Tammsalu et al., 2014) and ubiquitylated (Akimov et al., 2018; Kim et al., 2011; Lumpkin et al., 2017), with the latter being the most frequently reported modification (see Fig. 1D for potential post-translational modifications). These modifications might significantly affect the domain structure and function. In particular, ubiquitin-like protein 5 and SUMO-1 can be localized in CBs, and thus ubiquitylation and sumoylation can play an important role in CB integrity (Navascues et al., 2008; Sveda et al., 2013). Finally, coilin is strongly phosphorylated, and coilin phosphorylation modulates coilin interactions and CB formation (Cantarero et al., 2015; Carmo-Fonseca et al., 1993; Carrero et al., 2011; Hebert, 2013; Liu et al., 2000; Lyon et al., 1997; Sleeman et al., 1998). The K496E substitution might mimic phosphorylation and have a negative impact on CB integrity. Finally, we cannot exclude the possibility that the C-terminal coilin domain modulates coilin self-interaction, as suggested previously (Shpargel et al., 2003). Reduced self-association would be consistent with a lower residence time of EGFP–coilin^{K496E} in CBs (Fig. S1F).

Taken together, we identified and analyzed the K496E substitution in human coilin clones, which may well have been circulating in the scientific community via clones derived from the original plasmid deposited with the Addgene repository. Caution should be used, as the mutation might have influenced the ability of the protein to scaffold CBs especially in the absence of endogenous coilin.

MATERIALS AND METHODS
Cell culture
HeLa cells (ATCC® HeLa-CCL-2), HeLa^{coilinKO} cells (derived from parental HeLa cells, see below) and MEF$^{coilin-/-}$ cells (Tucker et al., 2001) were cultured in high-glucose (4.5 g/l) Dulbecco's modified Eagle's medium (DMEM, Sigma-Aldrich) supplemented with 10% fetal bovine serum (FBS, Gibco) and 1% penicillin/streptomycin (Gibco). MEF$^{coilin-/-}$ were kindly provided by Gregory Matera (University of North Carolina, Chapel Hill, USA) and previously characterized (Tucker et al., 2001).

CRISPR/Cas9 knockout cell line creation
The coilin knockout HeLa cell line was generated designing the guide RNA sequence to target the very N-terminus of coilin gene (first exon) using the online CRISPR Design Tool. Guide RNA was cloned into pX330-U6-Chimeric BB-CBh-hSpCas9 plasmid (Addgene #42230). To help sorting of possible positive cells, we cloned the guide target sequences into pARv-RFP reporter plasmid (Addgene #60021) (Kasparek et al., 2014). All products of cloning were confirmed by DNA sequencing. HeLa cells were grown to 90% confluency and co-transfected with pARv-RFP reporter plasmid and pX330 with guide RNA sequence using the Lipofectamine LTX transfection reagent (Thermo Fisher Scientific) according to the manufacturer's protocol. Cells were sorted 72 h after transfection for RFP positivity, one cell at a time, into the wells of 96-well plates containing a mixture of fresh and conditioned medium (1:1). Positive clones were selected by PCR using a set of primer directly prior and after the region target by guide RNA. Coilin expression was screened by immunofluorescence and western blotting.

Plasmid and transfection
EGFP–coilin and mRED–coilin (formally DsRed.M1-coilin) containing the mutations: c.784A>G (p.E251E), c.1642C>T (p.A537A) and c.1517A>G (p.K496E) were retrieved from our plasmid stocks. EGFP–coilin^{WT} was obtained by reverting the mutation c.1517A>G (p.K496E) by site-directed

mutagenesis using primers: 5′-AGGAAGGAAGAATATTAAGCCAC-3′ and 5′-TGTAGTCAGAGACATCAGGAGAG-3′. All tags were located at the N-terminus of coilin sequence. All constructs were verified by DNA sequencing.

Plasmids were transiently transfected into the cells with Lipofectamine LTX Transfection Reagent (Thermo Fisher Scientific) according to the manufacturer's instructions and cells analyzed 24 h post transfection.

Immunofluorescence and microscopy

For Fig. 1B, cells grown on coverslips were washed in PBS and fixed with 4% paraformaldehyde in PIPES for 10 min at 37°C. Coverslips were then washed in PBS and mounted in Fluoromount-G (Southern Biotech). For Fig. S1D, cells were permeabilized after fixation with 0.5% Triton X-100 for 5 min at room temperature (RT) and blocked in 5% bovine serum albumin. Subsequentially coverslips were stained with human auto-antibodies against fibrillarin (a kind gift of Dusan Cmarko, First Medical Faculty, Charles University in Prague, Czech Republic) diluted 1:1000 in PBS or the mouse monoclonal antibody against 2,2,7-trimethylguanosine (K121; Santa Cruz Biotechnology) diluted 1:50 in PBS for 1 h at RT. After a PBS wash, the coverslips were stained with goat anti-human-IgG secondary antibodies labeled with Alexa Fluor 594 (Thermo Fisher Scientific) or anti-mouse-IgG labeled with DyLight-549 (Jackson ImmunoResearch Laboratories) diluted 1:100 in PBS for 1 h RT. Coverslips were then washed in PBS and rinsed in distilled water. After being dried, they were mounted in Fluoromount-G. For Fig. 1B, primary antibody against FLAG (M2) mouse monoclonal IgG (F1804, Sigma) was utilized diluted 1:250 in PBS for 1 h at RT.

Images shown in Fig. 1B and Fig. S1B were acquired using a DMi8 inverted microscope with Leica confocal head TCS SP8 (Leica microsystems) equipped with a 63×/1.40 NA oil immersion objective and acquisition software LAS X (Leica microsystems). Stacks of 20–35 z-sections with 150 nm z-steps and 42 nm pixel size were taken per sample and maximum intensity projections are presented. Fig. 1C and Fig. S1C,D images were acquired using DeltaVision microscope system (Applied Precision Ltd.) coupled to the Olympus IX70 microscope equipped with a 60×/1.42 NA oil immersion objective, a CoolSNAP HQ2 camera (Photometrics; Princeton Instruments), and the acquisition software SoftWoRx (Applied Precision Ltd.). Stacks of 15–25 z-sections with 200 nm z-steps were taken per sample and maximum intensity projections are presented.

Quantification of cells with or without CBs was performed using DeltaVision microscope system coupled to the Olympus IX70 microscope equipped with a 60×/1.42 NA oil immersion objective. Cells were counted directly on the microscope and number of cells assayed is indicated in the graph (Fig. S1A).

FRAP

The FRAP experiment was performed on the DMi8 inverted microscope with Leica confocal head TCS SP8 equipped with a 63×/1.3 NA glycerol immersion objective corrected for use at 37°C and acquisition software LAS X. Cells were kept at 37°C and 5% CO2 for the whole imaging time. A 488-nm solid-state laser was used for both acquisition (0.2% laser intensity) and bleaching (25% laser intensity, single pulse, zoom-in mode). The following parameters were used for time-lapse acquisition: single focal plane, 62 nm pixel size, 2 lane accumulation and adaptive acquisition (152 ms interval for the first 100 frames, 300 ms for 75 frames and 600 ms for the last 80 frames). Owing to the lack of visible CBs in cells expressing a high level of EGFP–coilin^{K496E} FRAP analysis was limited to cells expressing low levels of EGFP–coilin for both constructs.

Western blotting

Cells cultivated in 10 cm Petri dishes were washed twice with ice-cold PBS, scraped from the dish, and centrifuged at 1000 g for 10 min at 4°C. Harvested cells were resuspended in NET-2 buffer (50 mM Tris-HCl pH 7.5, 150 mM NaCl, and 0.05% Nonidet P-40) supplemented with protease inhibitor cocktail (EMD) and RNase inhibitor (RNasin plus, Promega) then pulse sonicated on ice (30 pulses; 0.5 s for each pulse at 40% of maximum energy). The cell lysate was centrifuged at 14,000 g for 10 min at 4°C and the supernatant collected and diluted in 2× sample buffer. Subsequently,

proteins were separated by SDS-PAGE (10% gels) and transferred to a nitrocellulose membrane (Protran). Membranes were blocked with 5% nonfat milk (w/v) in PBS with 0.05% Tween-20 (PBST) and incubated with polyclonal anti-coilin rabbit IgG primary antibodies (H-300, Santa Cruz Biotechnology) diluted 1:2000 in 1% nonfat milk in PBST followed by PBST washes and incubation with anti-rabbit-IgG secondary antibodies conjugated to horseradish peroxidase (Jackson ImmunoResearch Laboratories) diluted 1:10,000 in 1% nonfat milk in PBST. Enzymatic activity was detected using the SuperSignal West Pico/Femto Chemiluminescent Substrate (Thermo Fisher Scientific).

Author contributions

Conceptualization: D.A.B., D.S.; Methodology: D.A.B.; Validation: D.A.B.; Investigation: D.A.B.; Writing - original draft: D.S.; Writing - review & editing: D.A.B., A.G.M.; Visualization: D.A.B.; Supervision: D.S.; Project administration: D.S.; Funding acquisition: D.A.B., A.G.M., D.S.

References

Akimov, V., Barrio-Hernandez, I., Hansen, S. V. F., Hallenborg, P., Pedersen, A. K., Bekker-Jensen, D. B., Puglia, M., Christensen, S. D. K., Vanselow, J. T., Nielsen, M. M. et al. (2018). UbiSite approach for comprehensive mapping of lysine and N-terminal ubiquitination sites. *Nat. Struct. Mol. Biol.* **25**, 631-640. doi:10.1038/s41594-018-0084-y

Andrade, L. E., Chan, E. K., Raska, I., Peebles, C. L., Roos, G. and Tan, E. M. (1991). Human autoantibody to a novel protein of the nuclear coiled body: immunological characterization and cDNA cloning of p80-coilin. *J. Exp. Med.* **173**, 1407-1419. doi:10.1084/jem.173.6.1407

Bohmann, K., Ferreira, J. A. and Lamond, A. I. (1995). Mutational analysis of p80 coilin indicates a functional interaction between coiled bodies and the nucleolus. *J. Cell Biol.* **131**, 817-831. doi:10.1083/jcb.131.4.817

Cajal, S. R. (1903). Un sencillo metodo de coloracion seletiva del reticulo protoplasmatico y sus efectos en los diversos organos nerviosos de vertebrados e invertebrados. *Trab. Lab. Invest. Biol. (Madrid)* **2**, 129-221.

Cantarero, L., Sanz-García, M., Vinograd-Byk, H., Renbaum, P., Levy-Lahad, E. and Lazo, P. A. (2015). VRK1 regulates Cajal body dynamics and protects coilin from proteasomal degradation in cell cycle. *Sci. Rep.* **5**, 10543. doi:10.1038/srep10543

Carmo-Fonseca, M., Ferreira, J. and Lamond, A. I. (1993). Assembly of snRNP-containing coiled bodies is regulated in interphase and mitosis–evidence that the coiled body is a kinetic nuclear structure. *J. Cell. Biol.* **120**, 841-852. doi:10.1083/jcb.120.4.841

Carrero, Z. I., Velma, V., Douglas, H. E. and Hebert, M. D. (2011). Coilin phosphomutants disrupt Cajal body formation, reduce cell proliferation and produce a distinct coilin degradation product. *PLoS ONE* **6**, e25743. doi:10.1371/journal.pone.0025743

Chan, E. K. L., Takano, S., Andrade, L. E. C., Hamel, J. C. and Matera, A. G. (1994). Structure, expression and chromosomal localization of human p80-coilin gene. *Nucleic Acids Res.* **22**, 4462-4469. doi:10.1093/nar/22.21.4462

Chen, Y., Deng, Z., Jiang, S., Hu, Q., Liu, H., Songyang, Z., Ma, W., Chen, S. and Zhao, Y. (2015). Human cells lacking coilin and Cajal bodies are proficient in

telomerase assembly, trafficking and telomere maintenance. *Nucleic Acids Res.* **43**, 385-395. doi:10.1093/nar/gku1277

Collier, S., Pendle, A., Boudonck, K., van Rij, T., Dolan, L. and Shaw, P. (2006). A distant coilin homologue is required for the formation of cajal bodies in Arabidopsis. *Mol. Biol. Cell.* **17**, 2942-2951. doi:10.1091/mbc.e05-12-1157

Hebert, M. D. (2013). Signals controlling Cajal body assembly and function. *Int. J. Biochem. Cell Biol.* **45**, 1314-1317. doi:10.1016/j.biocel.2013.03.019

Hebert, M. D. and Matera, A. G. (2000). Self-association of coilin reveals a common theme in nuclear body localization. *Mol. Biol. Cell* **11**, 4159-4171. doi:10.1091/mbc.11.12.4159

Hebert, M. D., Szymczyk, P. W., Shpargel, K. B. and Matera, A. G. (2001). Coilin forms the bridge between Cajal bodies and SMN, the spinal muscular atrophy protein. *Genes Dev.* **15**, 2720-2729. doi:10.1101/gad.908401

Kasparek, P., Krausova, M., Haneckova, R., Kriz, V., Zbodakova, O., Korinek, V. and Sedlacek, R. (2014). Efficient gene targeting of the Rosa26 locus in mouse zygotes using TALE nucleases. *FEBS Lett.* **588**, 3982-3988. doi:10.1016/j.febslet.2014.09.014

Kim, W., Bennett, E. J., Huttlin, E. L., Guo, A., Li, J., Possemato, A., Sowa, M. E., Rad, R., Rush, J., Comb, M. J. et al. (2011). Systematic and quantitative assessment of the ubiquitin-modified proteome. *Mol. Cell.* **44**, 325-340. doi:10.1016/j.molcel.2011.08.025

Liu, J., Hebert, M. D., Ye, Y., Templeton, D. J., Kung, H. and Matera, A. G. (2000). Cell cycle-dependent localization of the CDK2-cyclin E complex in Cajal (coiled) bodies. *J. Cell Sci.* **113**, 1543-1552. doi:10.1242/jcs.113.9.1543

Liu, J. L., Wu, Z., Nizami, Z., Deryusheva, S., Rajendra, T. K., Beumer, K. J., Gao, H., Matera, A. G., Carroll, D. and Gall, J. G. (2009). Coilin is essential for Cajal body organization in Drosophila melanogaster. *Mol. Biol. Cell* **20**, 1661-1670. doi:10.1091/mbc.e08-05-0525

Lumpkin, R. J., Gu, H., Zhu, Y., Leonard, M., Ahmad, A. S., Clauser, K. R., Meyer, J. G., Bennett, E. J. and Komives, E. A. (2017). Site-specific identification and quantitation of endogenous SUMO modifications under native conditions. *Nat. Commun.* **8**, 1171. doi:10.1038/s41467-017-01271-3

Lyon, C. E., Bohmann, K., Sleeman, J. and Lamond, A. I. (1997). Inhibition of protein dephosphorylation results in the accumulation of splicing snRNPs and coiled bodies within the nucleolus. *Exp. Cell Res.* **230**, 84-93. doi:10.1006/excr.1996.3380

Machyna, M., Neugebauer, K. M. and Staněk, D. (2015). Coilin: the first 25 years. *RNA Biol.* **12**, 590-596. doi:10.1080/15476286.2015.1034923

Navascues, J., Bengoechea, R., Tapia, O., Casafont, I., Berciano, M. T. and Lafarga, M. (2008). SUMO-1 transiently localizes to Cajal bodies in mammalian neurons. *J. Struct. Biol.* **163**, 137-146. doi:10.1016/j.jsb.2008.04.013

Raška, I., Andrade, L. E., Ochs, R. L., Chan, E. K., Chang, C. M., Roos, G. and Tan, E. M. (1991). Immunological and ultrastructural studies of the nuclear coiled body with autoimmune antibodies. *Exp. Cell Res.* **195**, 27-37. doi:10.1016/0014-4827(91)90496-H

Shanbhag, R., Kurabi, A., Kwan, J. J. and Donaldson, L. W. (2010). Solution structure of the carboxy-terminal Tudor domain from human Coilin. *FEBS Lett.* **584**, 4351-4356. doi:10.1016/j.febslet.2010.09.034

Shpargel, K. B., Ospina, J. K., Tucker, K. E., Matera, a. G. and Hebert, M. D. (2003). Control of Cajal body number is mediated by the coilin C-terminus. *J. Cell Sci.* **116**, 303-312. doi:10.1242/jcs.00211

Sleeman, J., Lyon, C. E., Platani, M., Kreivi, J. P. and Lamond, A. I. (1998). Dynamic interactions between splicing snRNPs, coiled bodies and nucleoli revealed using snRNP protein fusions to the green fluorescent protein. *Exp. Cell Res.* **243**, 290-304. doi:10.1006/excr.1998.4135

Stanek, D. (2017). Cajal bodies and snRNPs - friends with benefits. *RNA Biol.* **14**, 671-679. doi:10.1080/15476286.2016.1231359

Stanek, D. and Neugebauer, K. M. (2004). Detection of snRNP assembly intermediates in Cajal bodies by fluorescence resonance energy transfer. *J. Cell Biol.* **166**, 1015-1025. doi:10.1083/jcb.200405160

Stern, J. L., Zyner, K. G., Pickett, H. A., Cohen, S. B. and Bryan, T. M. (2012). Telomerase recruitment requires both TCAB1 and Cajal bodies independently. *Mol. Cell Biol.* **32**, 2384-2395. doi:10.1128/MCB.00379-12

Strzelecka, M., Trowitzsch, S., Weber, G., Lührmann, R., Oates, A. C. and Neugebauer, K. M. (2010). Coilin-dependent snRNP assembly is essential for zebrafish embryogenesis. *Nat. Struct. Mol. Biol.* **17**, 403-409. doi:10.1038/nsmb.1783

Sveda, M., Častoralova, M., Lipov, J., Ruml, T. and Knejzlík, Z. (2013). Human UBL5 protein interacts with coilin and meets the Cajal bodies. *Biochem. Biophys. Res. Commun.* **436**, 240-245. doi:10.1016/j.bbrc.2013.05.083

Tammsalu, T., Matic, I., Jaffray, E. G., Ibrahim, A. F. M., Tatham, M. H. and Hay, R. T. (2014). Proteome-wide identification of SUMO2 modification sites. *Sci. Signal.* **7**, rs2. doi:10.1126/scisignal.2005146

Tapia, O., Bengoechea, R., Berciano, M. T. and Lafarga, M. (2010). Nucleolar targeting of coilin is regulated by its hypomethylation state. *Chromosoma* **119**, 527-540. doi:10.1007/s00412-010-0276-7

Toyota, C. G., Davis, M. D., Cosman, A. M. and Hebert, M. D. (2010). Coilin phosphorylation mediates interaction with SMN and SmB'. *Chromosoma* **119**, 205-215. doi:10.1007/s00412-009-0249-x

Tucker, K. E., Massello, L. K., Gao, L., Barber, T. J., Hebert, M. D., Chan, E. K. and Matera, A. G. (2000). Structure and characterization of the murine p80 coilin gene, Coil. *J. Struct. Biol.* **129**, 269-277. doi:10.1006/jsbi.2000.4234

Tucker, K. E., Berciano, M. T., Jacobs, E. Y., LePage, D. F., Shpargel, K. B., Rossire, J. J., Chan, E. K. L., Lafarga, M. and Conlon, R. A. (2001). Residual Cajal bodies in coilin knockout mice fail to recruit Sm snRNPs and SMN, the spinal muscular atrophy gene product. *J. Cell Biol.* **154**, 293-308. doi:10.1083/jcb.200104083

Tuma, R. S., Stolk, J. A. and Roth, M. B. (1993). Identification and characterization of a sphere organelle protein. *J. Cell Biol.* **122**, 767-773. doi:10.1083/jcb.122.4.767

Wu, Z., Murphy, C. and Gall, J. G. (1994). Human p80-coilin is targeted to sphere organelles in the amphibian germinal vesicle. *Mol. Biol. Cell* **5**, 1119-1127. doi:10.1091/mbc.5.10.1119

Xu, H., Pillai, R. S., Azzouz, T. N., Shpargel, K. B., Kambach, C., Hebert, M. D., Schümperli, D. and Matera, A. G. (2005). The C-terminal domain of coilin interacts with Sm proteins and U snRNPs. *Chromosoma* **114**, 155-166. doi:10.1007/s00412-005-0003-y